Scientific Research Publishing

Journal of Materials Science and Chemical Engineering, 2017, 5, 19-28
http://www.scirp.org/journal/msce
ISSN Online: 2327-6053
ISSN Print: 2327-6045

Finite Element Analysis of Graphite/Epoxy Composite Pressure Vessel

Meng-Kao Yeh, Tai-Hung Liu

Department of Power Mechanical Engineering, National Tsing Hua University, Taiwan
Email: mkyeh@pme.nthu.edu.tw

How to cite this paper: Yeh, M.-K. and Liu, T.-H. (2017) Finite Element Analysis of Graphite/Epoxy Composite Pressure Vessel. *Journal of Materials Science and Chemical Engineering*, **5**, 19-28.
https://doi.org/10.4236/msce.2017.57003

Received: April 13, 2017
Accepted: July 4, 2017
Published: July 7, 2017

Abstract

Shell structure is widely used in industrial applications, such as in machinery, aerospace, ship and building fields, as well as containers of pressurized chemicals or liquefied natural gas. Graphite/epoxy composites has advantages of light weight, high strength, corrosion resistance, low expansion, low shrin kage and are often used in the form of composite pressure vessel for various engineering applications. In this study, the stress distributions of composite pressure vessel were analyzed. The finite element code ANSYS was used in analysis, in which the eight-node element SHELL 281 was adopted. The internal pressure 20 MPa, as in container of compressed natural gas, was applied inside the symmetrical cross-ply graphite/epoxy composite pressure vessel. The finite element model was established with suitable mesh size and boundary conditions. The stress distributions are discussed for the composite pressure vessel, especially for the inner two layers at the junction of semis pherical part. The Tsai-Hill criterion was used to assess the failure of composite pressure vessel.

Keywords

Finite Element Analysis, Stress Analysis, Composite Pressure Vessel, Tsai-Hill Failure Criterion

1. Introduction

Composite pressure vessels provide substantial weight reduction, high impact strength, zero corrosion and longer fatigue life, when compared with common metal ones. The composite pressure vessels can be used to carry compressed natural gas (CNG). CNG, mainly composed of methane (CH_4), is compressed to 20 MPa in high pressure cylinders operated at minus 40 to 60 degrees Celsius [1] [2]. After decompression, CNG is supplied for combustion to achieve power as a high quality alternative fuel for automobiles. CNG has the advantages of good

anti-blast performance, less emissions of harmful substances, extended service life and reduced fuel costs. Yen [3] mentioned that discontinuous stress and bending stress occurred at the junction of semispherical part of pressure vessel. Yue and Li [1] used high-density polyethylene (HDPE) as the liner of composite pressure vessel to cover the cylinder up to the junction of end plate to avoid failure.

In this study, the composite pressure vessel is analyzed using finite element method. The symmetrical cross-ply composite pressure vessel model with different boundary conditions is analyzed and its stress distribution and failure behavior assessed by Tsai-Hill criterion are discussed for the composite pressure vessel.

2. Composite Shell Analysis

2.1. First-Order Shear Deformation Theory (FSDT)

The composite pressure vessel is assumed to be an intermediately thick shell structure, with thickness/cylindrical radius greater than 0.18. The first-order shear deformation theory (FSDT) proposed by Mindlin [4] assumed a constant transverse shear deformation through the intermediately thick shell. The element type –8 node Shell 281 [5] [6] used in finite element analysis is based on FSDT in this study. As shown in **Figure 1**, the coordinate system α-β is at the middle surface of shell, and the z-axis is in the thickness direction of shell. Assuming no normal strain, $\varepsilon_z = 0$, the normal of shell keeps straight during deformation, but not perpendicular to the middle surface. The displacement field can be expressed as

$$\begin{aligned} u(\alpha,\beta,z) &= u_0(\alpha,\beta) + z\psi_\alpha(\alpha,\beta) \\ v(\alpha,\beta,z) &= v_0(\alpha,\beta) + z\psi_\beta(\alpha,\beta) \\ w(\alpha,\beta,z) &= w_0(\alpha,\beta) \end{aligned} \tag{1}$$

where u_0, v_0, w_0 represent the displacement at middle surface of shell. ψ_α and ψ_β are the mid-surface rotations.

The stress and strain relationship of k-th layer of composite laminate is shown below [7].

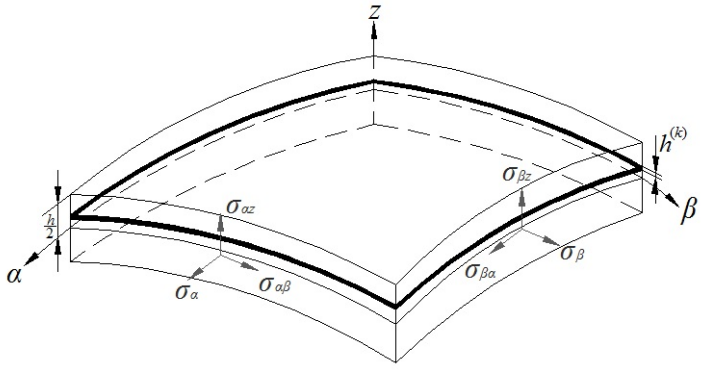

Figure 1. Shell's α-β-z coordinate system.

$$\begin{bmatrix} \sigma_{\alpha}^{k} \\ \sigma_{\beta}^{k} \\ \sigma_{\beta z}^{k} \\ \sigma_{\alpha z}^{k} \\ \sigma_{\alpha\beta}^{k} \end{bmatrix} = \begin{bmatrix} \overline{Q_{11}} & \overline{Q_{12}} & 0 & 0 & \overline{Q_{16}} \\ \overline{Q_{12}} & \overline{Q_{22}} & 0 & 0 & \overline{Q_{26}} \\ 0 & 0 & \overline{Q_{44}} & \overline{Q_{45}} & 0 \\ 0 & 0 & \overline{Q_{45}} & \overline{Q_{55}} & 0 \\ \overline{Q_{16}} & \overline{Q_{26}} & 0 & 0 & \overline{Q_{66}} \end{bmatrix} \begin{Bmatrix} \varepsilon_{\alpha}^{k} \\ \varepsilon_{\beta}^{k} \\ \gamma_{\beta z}^{k} \\ \gamma_{\alpha z}^{k} \\ \gamma_{\alpha\beta}^{k} \end{Bmatrix} \tag{2}$$

The coefficient of stiffness matrix ($\overline{Q_{ij}}$) is obtained after transforming the stiffness matrix from the material principal axis to α-β axis, as shown in Equation (3) [7], in which c and s represent $cos\theta$ and $sin\theta$ respectively.

$$\begin{aligned} \overline{Q_{11}} &= Q_{11}c^4 + 2\left(Q_{12} + 2Q_{66}\right)c^2s^2 + Q_{22}s^4 \\ \overline{Q_{12}} &= \left(Q_{11} + Q_{22} - 4Q_{66}\right)c^2s^2 + Q_{12}(c^4 + s^4) \\ \overline{Q_{16}} &= -cs^3Q_{22} + c^3sQ_{11} - cs(c^2 - s^2)(Q_{12} + 2Q_{66}) \\ \overline{Q_{22}} &= Q_{11}s^4 + 2\left(Q_{12} + 2Q_{66}\right)c^2s^2 + Q_{22}c^4 \\ \overline{Q_{26}} &= cs^3Q_{11} - c^3sQ_{22} - cs\left(c^2 - s^2\right)(Q_{12} + 2Q_{66}) \\ \overline{Q_{44}} &= Q_{44}c^2 + Q_{55}s^2 \\ \overline{Q_{45}} &= \left(Q_{55} - Q_{44}\right)cs \\ \overline{Q_{55}} &= Q_{55}c^2 + Q_{44}s^2 \\ \overline{Q_{66}} &= (Q_{11} + Q_{22} - 2Q_{12})c^2s^2 + Q_{66}\left(c^2 - s^2\right)^2 \end{aligned} \tag{3}$$

The coefficients of stiffness matrix (Q_{ij}) are expressed below [7].

$$Q_{11} = E_{11}\frac{1-\upsilon_{23}\upsilon_{32}}{\Delta}, Q_{12} = E_{11}\frac{\upsilon_{21}+\upsilon_{31}\upsilon_{23}}{\Delta} = E_{22}\frac{\upsilon_{12}+\upsilon_{32}\upsilon_{13}}{\Delta}, Q_{22} = E_{22}\frac{1-\upsilon_{31}\upsilon_{13}}{\Delta},$$
$$Q_{44} = G_{23}, Q_{55} = G_{13}, Q_{66} = G_{12}, \Delta = 1-\upsilon_{12}\upsilon_{21}-\upsilon_{23}\upsilon_{32}-\upsilon_{31}\upsilon_{13}-2\upsilon_{21}\upsilon_{32}\upsilon_{13} \tag{4}$$

where E_{11} and E_{22} are the Young. s modulus of composites in three directions; G_{12}, G_{23} and G_{13} are the shear modulus; υ_{12}, υ_{23} and υ_{13} are the Poisson's ratio of composites.

2.2. Tsai-Hill Failure Criterion

In this study, the composite pressure vessel is under the operating internal pressure 20 MPa. The Tsai-Hill failure criterion was used through the thickness of the pressure vessel to determine whether the pressure vessel fails or not. The Tsai-Hill failure criterion is expressed as [8]

$$\frac{\sigma_1^2}{S_L^2} - \frac{\sigma_1\sigma_2}{S_L^2} + \frac{\sigma_2^2}{S_T^2} + \frac{\tau_{12}^2}{S_{LT}^2} \geq 1 \tag{5}$$

where σ_1 is the stress in the fiber direction, σ_2 the transverse stress and τ_{12} the shear stress. S_L and S_T are the tensile strengths in the fiber and transverse directions and S_{LT} the shear strength for the composite lamina. When Equation (5) is true, it represents the possible failure at some layer in the composite pressure vessel. In the latter section, the value of left hand side of Equation (5) is termed as Tsai-Hill criterion value, which indicates failure of composite pressure vessel

when this value is greater than 1.

3. Finite Element Analysis

3.1. The Composite Pressure Vessel

The composite pressure vessel has overall length 808 mm with a central cylinder part 592.5 mm, as shown in **Figure 2**. The outside diameter of central composite section is 215.5 mm. The opening diameter of end plate is 40 mm. The thickness of composite pressure vessel is 18 mm, which is formed by a total of 144 graphite/epoxy composite layers; each layer has a thickness of 0.125 mm. The laminate stacking of composite pressure vessel is symmetrical cross-ply, $[(0/90)_s]_{36}$, counting from inside wall as layer 1 with fiber in the hoop direction. In **Figure 3**, the schematic of selected inner and outer layers is shown.

3.2. Material Properties

The material properties of graphite/epoxy composites are given below in **Table 1** and **Table 2** [9] [10]. The graphite/epoxy composite lamina is assumed to be specially orthotropic $\upsilon_{12} = \upsilon_{13} = \upsilon_{23}$, $E_{22} = E_{33}$, $G_{23} = E_{22}/2(1 + \upsilon_{23})$ [8], since υ_{13}, υ_{23}, E_{33} are difficult to be measured.

The longitudinal and transverse strengths of graphite/epoxy composite lamina are adopted from [10] and the shear strength is from [9].

3.3. Internal Pressure Load and Boundary Conditions

The operating internal pressure of composite pressure vessel is 20 MPa with compressed natural gas (CH_4) at minus 40 to 60 degrees Celsius [1] [2]. Two types of boundary conditions, clamped by buckles as the first type and free ex-

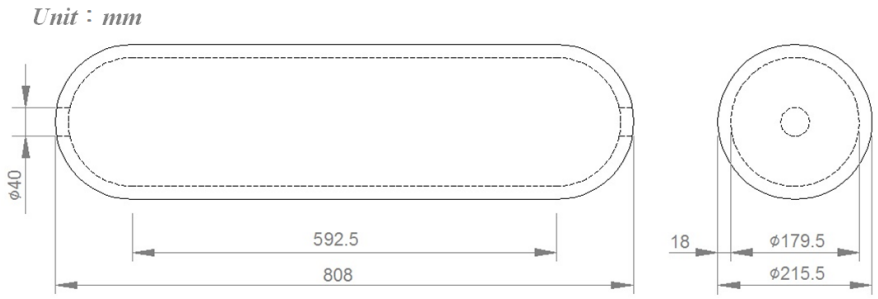

Figure 2. Dimensions of composite pressure vessel.

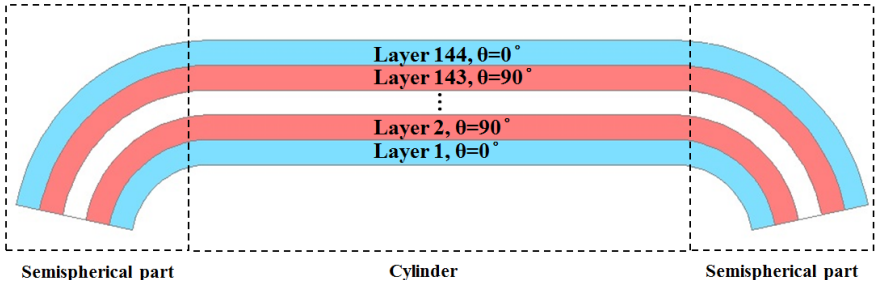

Figure 3. Schematic of selected layers.

Table 1. Young's modulus, Poission ratio and shear modulus of graphite/epoxycomposites [9].

E_{11} (GPa)	E_{22} (GPa)	E_{33} (GPa)	υ_{12}	υ_{13}	υ_{23}	G_{12} (GPa)	G_{13} (GPa)	G_{23} (GPa)
128.484	9.135	9.135	0.249	0.249	0.249	5.705	5.705	3.66

Table 2. Strength of graphite/epoxy composites.

S_L (MPa)	S_T (MPa)	S_{LT} (MPa)
2266 [10]	70 [10]	84.108 [9]

pansion as the second type, are prescribed at the junction of semispherical part in analysis, as shown in **Figure 4**. The two end plates are placed at both ends to restrict all axial degrees of freedom (DOFs).

3.4. Analysis Model of Composite Pressure Vessel

The commercial finite element code ANSYS [5] was used in analysis. The composite pressure vessel is meshed using 8-node element, Shell 281 [5] [6]. The stress at a selected point at the junction of semispherical part was calculated with different element numbers. **Figure 5** shows the analysis model and convergence analysis of composite pressure vessel. The difference of simulated results at selected point is less than 1% for the analysis model of composite pressure vessel with 22,400 elements and 67,456 nodes. This analysis model is used for the rest of this study.

4. Results and Discussion

The stress distribution of composite pressure vessel was analyzed. The value of Tsai-Hill criterion was calculated to evaluate the failure of composite pressure vessel under operating internal pressure 20 MPa [1] [2] with two types of boundary conditions. For the first type boundary condition, all DOFs at two junctions of semispherical parts are all prescribed to be zero and prescribed to be free for the second type boundary condition. Due to the symmetry of pressure vessel, the stresses are the same in the hoop direction. **Figure 6** shows the designated curve to calculate the stresses and the values of Tsai-Hill criterion for discussion.

4.1. Results of Stress Distribution

Since the layer 1 directly contacts with the internal pressure loading, the stresses in the fiber and transverse directions for layer 1 and 2, relatively large when compared with the stresses in other layers, are of primary concern and are discussed in the following sections. **Figure 7** and **Figure 8** show the von Mises stress distributions of layer 1 and layer 2 of composite pressure vessel with first type and second type boundary conditions. The von Mises stress values are in the range of 80 - 100 MPa. In the cylindrical part, the stress is very high in layer 1, 163 - 180 MPa, and very small in layer 2.4.5 - 24.1 MPa in the cylindrical part

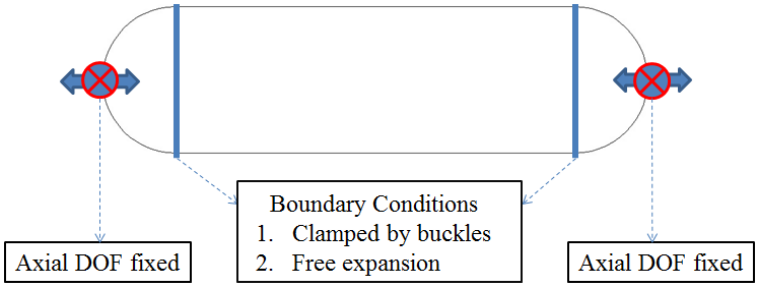

Figure 4. Boundary condition of composite pressure vessel.

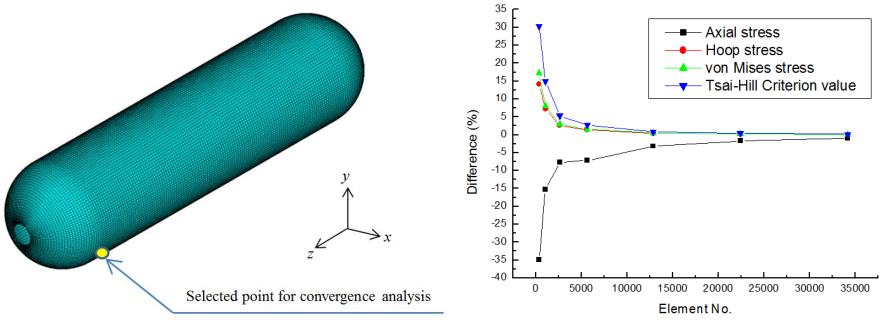

(a) (b)

Figure 5. Analysis model and convergence analysis of composite pressure vessel. (a) Analysis model; (b) Convergence analysis.

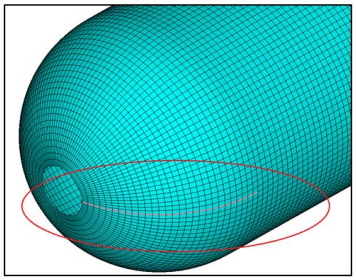

Figure 6. The designated curve to calculate stresses and values of Tsai-Hillcriterion.

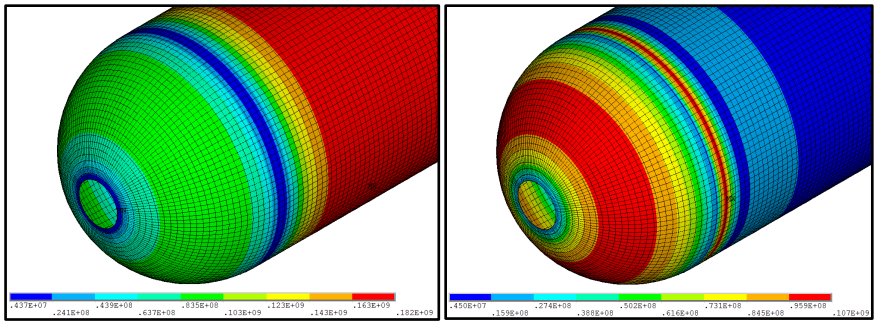

(a) (b)

Figure 7. Von Mises stress distributions of composite pressure vessel under first type boundary condition. (a) Layer 1; (b) Layer 2.

for both boundary conditions. At the junction of semispherical part, von Mises stress is 106.34 MPa for layer 1 and 98.408 MPa for layer 2 under first type

boundary condition; von Mises stress is 84.64 MPa for layer 1 and 92.531 MPa for layer 2 under second type boundary condition.

The stresses in the fiber and transverse directions of composite lamina are obtained by transforming the stress components from finite element analysis in the α-β coordinate system. First the discussion for the stresses in composite pressure vessel is simply based on the maximum stress criterion. The shear stresses obtained are very small and negligible when compared with the shear strength of graphite/epoxy composites. The stresses in the fiber and transverse directions for layer 1 and layer 2 along the designated curve for first type boundary condition are shown in **Figure 9**. In **Figure 9(a)**, the stress of layer 1 in the fiber direction σ_1 at the junction is 108.23 MPa, much lower than the corresponding material strength 2200 MPa; the stress in the transverse direction σ_2 is 3.89 MPa, lower than the corresponding material strength 70 MPa. Therefore no failure occurs in layer1 for the composite pressure vessel under first type boundary condition. However, in **Figure 9(b)**, the stress of layer 2 in the fiber directionσ_1 at the junction is 4.87 MPa, much lower than the corresponding material strength 2200 MPa and the stress in the transverse direction σ_2 is 100.75 MPa, larger than the corresponding material strength 70 MPa. Therefore failure may occur in layer2 for the composite pressure vessel under first type boundary condition.

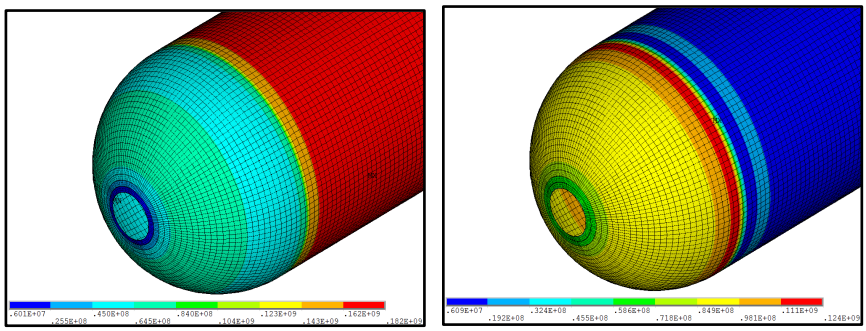

(a) (b)

Figure 8. Von Mises stress distribution of composite pressure vessel under second type boundary condition. (a) Layer 1; (b) Layer 2.

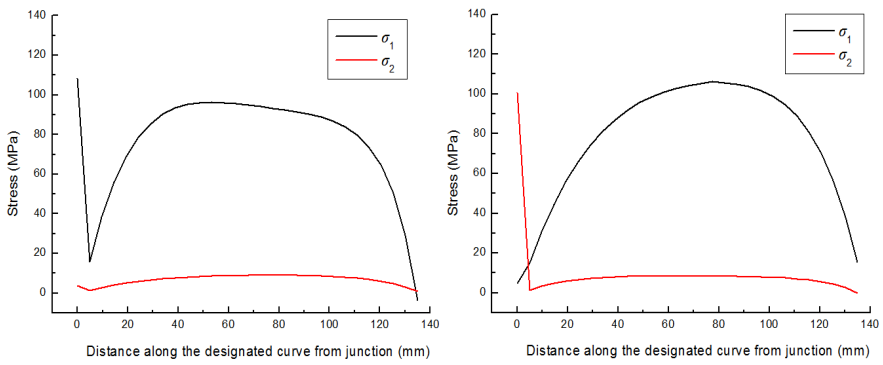

(a) (b)

Figure 9. The stress along the designated curve for first type boundary condition. (a) Layer 1; (b) Layer 2.

The stresses in the fiber and transverse directions for layer 1 and 2 along the designated curve for second type boundary condition are shown in **Figure 10**. In **Figure 10(a)**, the stress of layer 1 in the fiber directionσ_1 at the junction is 55.915 MPa and maximum 70.692 MPa, much lower than the corresponding material strength 2200 MPa; the stress in the transverse direction σ_2 is 94.934 MPa, larger than the corresponding material strength 70 MPa. Therefore failure may occur in layer1 for the composite pressure vessel under second type boundary condition. In **Figure 10(b)**, the stress of layer 2 in the fiber directionσ_1 at the junction is 95.99 MPa and maximum 127.51 MPa, much lower than the corresponding material strength 2200 MPa and the stress in the transverse direction σ_2 is 6.44 MPa, also lower than the corresponding material strength 70 MPa. Therefore no failure occurs in layer 2 for the composite pressure vessel under second type boundary condition.

4.2. Results of Tsai-Hill Failure Criterion

The results from the previous section show that the stress in the transverse direction is the main reason for failure of composite pressure vessel since the stress is greater than its corresponding strength 70 MPa, based on the maximum stress criterion. The Tsai-Hill criterion, Equation (5), is also used to assess the failure of composite pressure vessel for both types of boundary conditions. **Figure 11** shows the Tsai-Hill criterion value of layer 1 and 2 along the designated curve from junction. From **Figure 11(a)**, the Tsai-Hill criterion value of layer 2 is 2.07, greater than 1; this indicates the failure of layer 2 in composite pressure vessel under first type boundary condition. On the contrary from **Figure 11(b)**, the Tsai-Hill criterion value of layer 1 is 1.84, greater than 1; this indicates the failure of layer 1 in composite pressure vessel under second type boundary condition.

5. Conclusion

In this study, the stress distributions of symmetrical cross-ply graphite/epoxy composite pressure vessel under internal pressure 20 MPa were analyzed using finite element method. Two types of boundary conditions were considered in

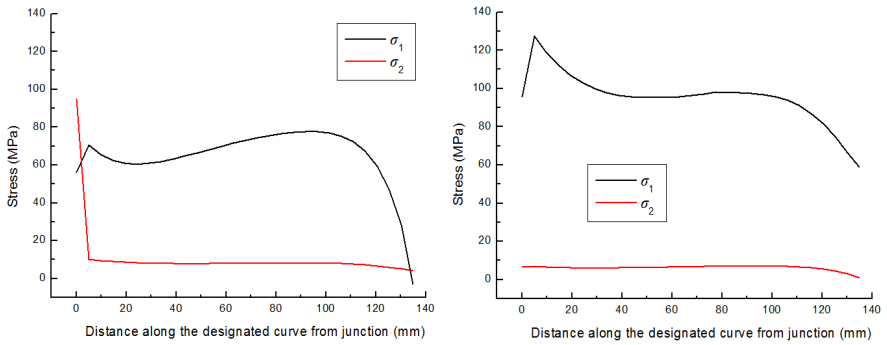

Figure 10. The stress along the designated curve forsecond type boundary condition. (a) Layer 1; (b) Layer 2.

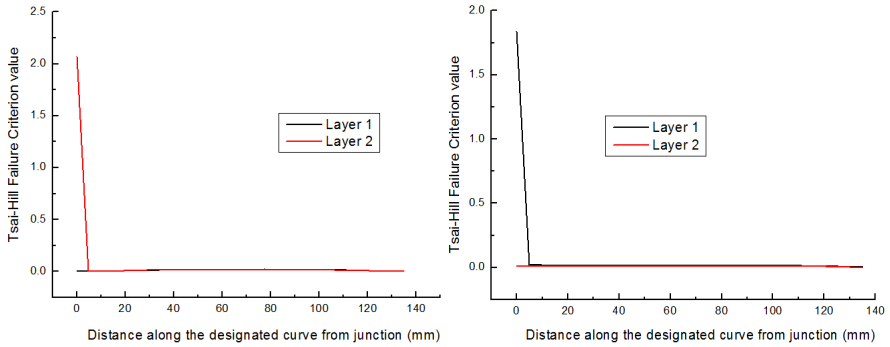

Figure 11. Tsai-Hill criterion value along the designated curve. (a) First type boundary condition; (b) Second type boundary condition.

analysis. The Tsai-Hill criterion was used to assess the failure of composite pressure vessel. The stress distribution and Tsai-Hill failure criterion are discussed for the inner two layers of composite pressure vessel at the junction of semispherical part. It can be concluded that layer 2 failure occurred for the composite pressure vessel studied under first type boundary condition; while layer 1 failed for the composite pressure vessel under second type boundary condition.

Acknowledgements

The authors would like to thank the support from Ministry of Science and Technology, Taiwan through the grant MOST 105-2221-E-007-031-MY3. The support is greatly acknowledged.

References

[1] Yue, Z.Z. and Li, X. (2012) Numerical Simulation of All-Composite Compressed Natural Gas (CNG) Cylinders for Vehicle. *Procedia Engineering*, **37**, 31-36. https://doi.org/10.1016/j.proeng.2012.04.197

[2] Nirbhay, M., Juneja, S., Dixit, A., Misra, R.K. and Sharma, S. (2015) Finite Element Analysis of All Composite CNG Cylinders. *Procedia Materials Science*, **10**, 507-512. https://doi.org/10.1016/j.mspro.2015.06.093

[3] Yen, H.Y. (2013) Structural Analysis and Evaluation of Pressure Vessel Supports. Master's Thesis, National Cheng Kung University, Tainan.

[4] Mindlin, R.D. (1951) Influence of Rotatory Inertia and Shear Deformation on Flexural Motion of Isotropic, Elastic Plates. *Journal of Applied Mechanics*, **18**, 31-38.

[5] ANSYS Release 12.1 (2009) ANSYS, Inc., PA.

[6] ANSYS User's Manual, ANSYS Inc.

[7] Qatu, M.S. (2004) Vibration of Laminated Shells and Plates. 1st Edition, Elsevier Ltd., Amsterdam.

[8] Gibson, R.F. (2007) Principles of Composite Material Mechanics.2nd Edition, CRC Press Ltd., U.S.

[9] Liu, T.H. and Yeh, M.K.(2016) Finite Element Analysis of Quasi-Isotropic Carbon/Epoxy Composite Hemispherical Shell. *The 40th National Conference on*

Theoretical and Applied Mechanics, Hsinchu, 25-26 November 2014, Article ID: No. 1168.

[10] AD Group-P (2016). High Performance Structural Application. Advanced International Multitech Co., Ltd.